Magnetism and clustering in Cr-doped InN

A. Belabbes, A. Zaoui, and M. Ferhat

Citation: Applied Physics Letters **97**, 242509 (2010); doi: 10.1063/1.3527978
View online: http://dx.doi.org/10.1063/1.3527978
View Table of Contents: http://scitation.aip.org/content/aip/journal/apl/97/24?ver=pdfcov
Published by the AIP Publishing

Magnetism and clustering in Cr-doped InN

A. Belabbes,[1] A. Zaoui,[2,a)] and M. Ferhat[1]
[1]*Département de Physique, LEPM, Université des Sciences et de la Technologie d'Oran, 31000 Oran, Algeria*
[2]*LGCgE-EA 4515, Lille Nord de France, Polytech'Lille, Université de Lille 1, 59655 Villeneuve D'Ascq, France*

(Received 1 September 2010; accepted 19 November 2010; published online 17 December 2010)

Density functional theory was applied to study the electronic and magnetic coupling of Cr-doped InN, in which magnetic configurations have been investigated. We found that the calculated ferromagnetic stabilizing energy is strongly linked to the Cr–Cr distance. The local magnetic moment of Cr is $2.3\mu_B$, and it weakly depends on the Cr–Cr distance. The coupling between the Cr *d* and the N *p* states is found to be the origin of ferromagnetism in the InCrN system. The generalized gradient approximation-1/2 correction procedure increases the polarization of InCrN, making this system a robust half-metallic ferromagnetic alloy. © *2010 American Institute of Physics*. [doi:10.1063/1.3527978]

Dilute magnetic semiconductor (DMS) materials are semiconductors doped by magnetic transition metal ions. They have attracted intense interest as promising candidates for future generation of multifunctional spintronic devices.[1] The manipulation of the electron spin in semiconducting devices will improve the conventional semiconductor technology.

InMnAs and GaMnAs were the earliest ferromagnetic DMS materials discovered by Munekata *et al.*[2] and Ohno *et al.*[3] but with Curie temperature below room temperature. For practical applications, DMS must be achieved with temperature higher than room temperature. One methodology for enhancing the Curie temperature is to use smaller bond length materials with lower spin-orbit coupling, as would be found in transition metal-doped nitrides. The theoretical study of Dhar *et al.*[4] predicted high Curie temperatures for wide band gap semiconductor, suggesting a promising possibility of these materials for spintronic device applications. Ferromagnetic III-nitride semiconductors would provide complementary functionality to the wide range of commercial devices already developed in wide gap system. Experimental studies confirmed room temperature ferromagnetism in a number of materials, including GaMnN,[4] GaCrN,[5] AlCrN,[6] GaGdN,[7] and AlFeN.[8] Recently, several research groups[9–13] found that InN-doped Cr shows magnetic order above room temperature. Chen *et al.*[9] observed ferromagnetism above room temperature in $In_{0.98}Cr_{0.02}N$ film. Moreover, Ney and co-workers[10,12,13] observed ferromagnetism behavior up to 300 K for small Cr compositions. On the other hand, recent experimental results[14] show that InN-doped Cr does not compare well with conventional ferromagnets but show a metastable behavior. On the theoretical side, relatively limited theoretical analysis[15] on the Cr-doped InN has been reported.

The electronic and magnetic properties have been computed using the spin-polarized density functional theory based on generalized gradient approximation functional in the form of Perdew–Burke–Ernzherof[16] for the exchange and correction potentials, which are implemented in QUANTUM-ESPRESSO software package.[17] Brillouin zone integrations were performed by using $4\times4\times4$ Monkhorst and Pack special point[18] and Marzari–Vanderbilt smearing technique[19] with a smearing width of 0.02 Ry. The wave functions were expanded in plane waves up to cutoff energies of 30 and 200 Ry for charge density and potential. A large 64 atom supercell representation is used in order to model the InNCr alloys. More specifically, for the 64 atom InNCr supercells, which correspond to $2\times2\times2$ conventional cubic cells, a zinc blende lattice is assumed. The forces acting on each atom are determined using a variation of the Hellmann–Feynman theorem.[20,21]

To study the magnetic coupling between Cr atoms, we have replaced a pair of In atoms with Cr atoms at different sites to simulate the Cr-doped InN. This replacement corresponds to a doping composition of 6.25%, which is closer to the experimental values. Recent experiment of Anderson *et al.*[11] suggested that Cr atoms occupy substitutional sites. Therefore, there are many ways to model this substitution, depending on the sites where Cr atoms are distributed. We consider four different configurations (C_1, C_2, C_3, and C_4), which correspond to four different separations in increasing order between two Cr atoms. We begin with a minimum Cr–Cr distance configuration (i.e., C_1) and then we sequentially move the Cr atom to finally generate a maximum Cr–Cr distance configuration (i.e., C_4).

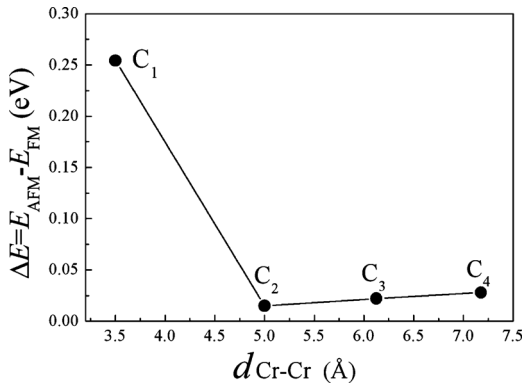

FIG. 1. The total energy difference ΔE between ferromagnetic and antiferromagnetic configurations vs Cr–Cr distance *d* in the unit cell.

a)Electronic mail: azaoui@polytech-lille.fr.

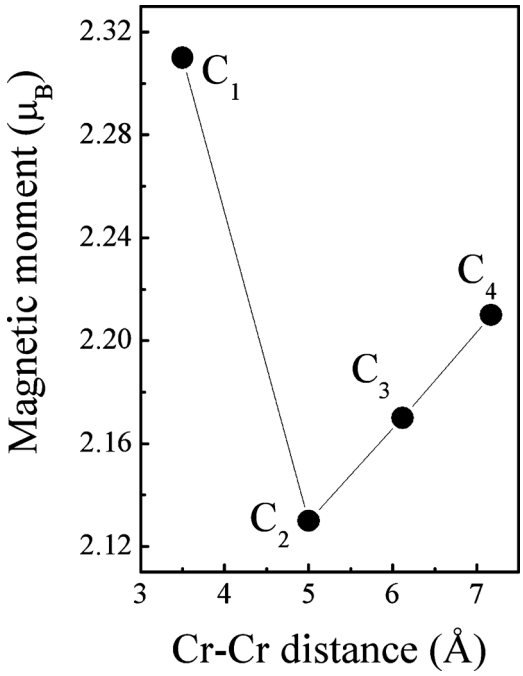

FIG. 2. Magnetic local moment of Cr vs Cr–Cr distances d.

The total energies corresponding to both FM and AFM spin alignments for all the configurations were calculated to determine the preferred geometric and magnetic moments located at each Cr atom self-consistently. Figure 1 shows our calculated pairwise ferromagnetic stabilization energy $\Delta E = E_{AFM} - E_{FM}$ as a function of the Cr–Cr separation d, where E_{FM} and E_{AFM} are the total energies of ferromagnetic and antiferromagnetic pairs, respectively, with the Cr–Cr distance up to 7.17 Å.

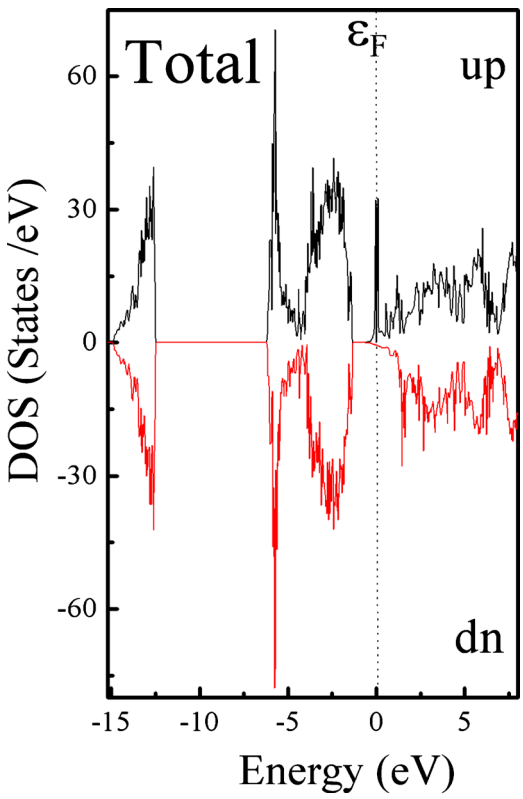

FIG. 3. (Color online) The total DOS of $In_{30}Cr_2N_{32}$ supercell for majority spin (top) and minority spin (bottom). The Fermi level is set at zero.

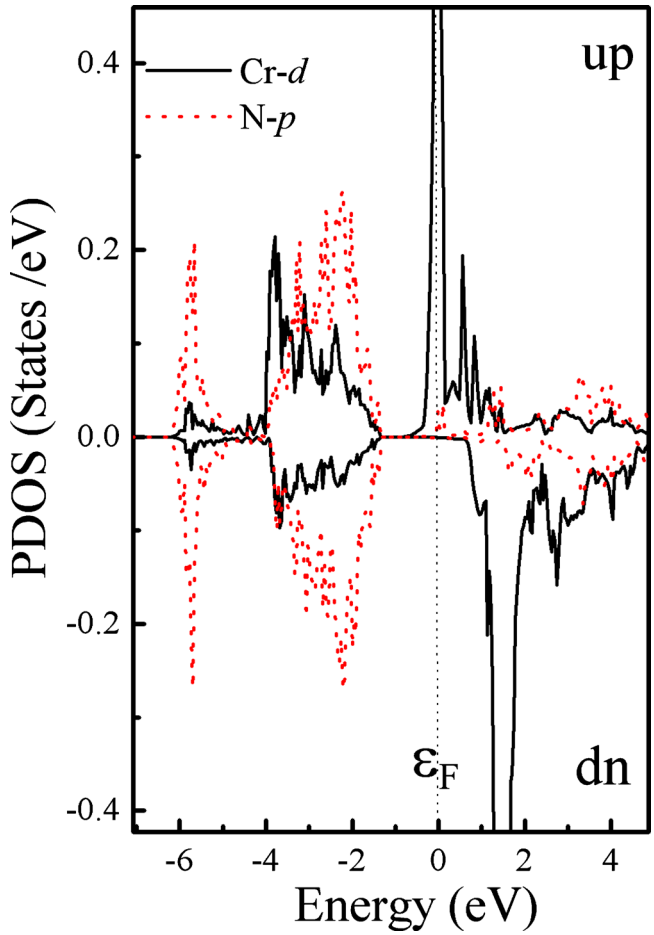

FIG. 4. (Color online) The partial PDOS of Cr 3d (straight lines) and the neighboring N 2p (dot line) states. The Fermi level is set at zero.

We observe that the ferromagnetic interaction between Cr spins is favored for all the cases considered here. The first nearest neighbor exchange interaction with the Cr–Cr separation of 3.50 Å is the strongest with a lowering of energy by 254 meV compared to the antiferromagnetic configuration. It is also noticed from Fig. 1 that ΔE decreases sharply with the increase of Cr–Cr distances. For the separate configurations, we find that all three configurations C_2, C_3, and C_4 are nearly degenerate in energy, about 15, 22, and 27 meV, respectively, which shows that ferromagnetic exchange interaction between magnetic dopants have a tendency for the formation of Cr clusters within a short radial distance. It is also clear that for large Cr–Cr separation (i.e., C_2, C_3, and C_4), the system tends to stabilize in an AFM ground state (but the system is still FM), which implies that the AFM exchange interaction is long ranged. Moreover, we notice a weak dependence of ΔE with the Cr–Cr separation for the far configurations.

The dependence of local magnetic moment (LMM) of Cr atom as a function of the Cr–Cr distance is shown in Fig. 2. The highest LMM of Cr is $2.3\mu_B$ for the C_1 configuration, which corresponds to the highest FM stability energy. While the minimum LMM of Cr corresponds to the C_2 configuration characterized by the lowest FM stability energy. Furthermore, it is seen that the magnetic moment does not show much variation depending on the distance for all the geometries, which is an indication that the direct interaction between the Cr atoms is minimal.

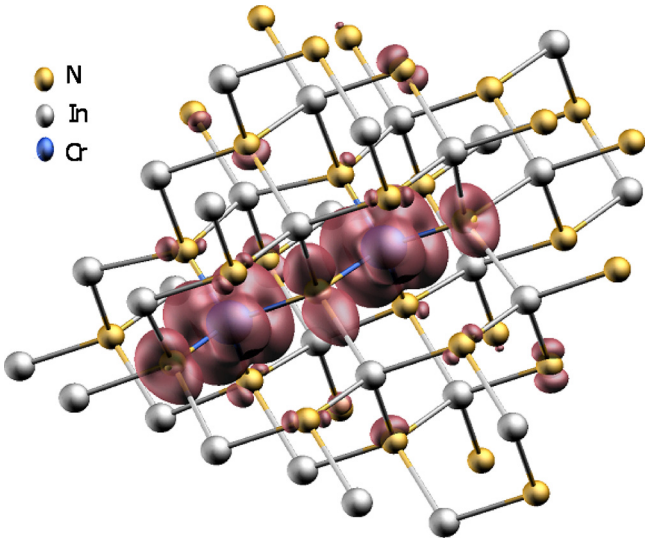

FIG. 5. (Color online) Partial charge density plot for majority spin close to the Fermi level.

We address now the magnetic properties of InCrN alloy for the C_1 configuration. A well-known problem of generalized gradient approximation (GGA) is the underestimation of the band gap of nonmetal compounds; this failure is severe for InN (Ref. 22) and, consequently, for the InCrN system where the Cr and N valence bands can be erroneously found mixed with conduction bands. In order to overcome this problem, we apply [density functional theory (DFT)/GGA]-1/2 method[23] by using VASP.[24] This approach meets a precision similar to that of the *GW* approximation,[25] which attempts to fix the electron self-energy deficiency of DFT. We used the Perdew–Burke–Ernzherof form of GGA, the wave functions were expanded in plane waves up to a cutoff energy of 40 Ry and Brillouin zone integrations were performed by using a $4\times4\times4$ Monkhorst and Pack special point grids.

Instead of the metallic character found without correction, the GGA-1/2 improves significantly the band gap of InN. We found a band gap of 0.537 eV, which is in good agreement with recent experiment[26] and theoretical works.[22] The total density of states (DOS) and the partial DOS of Cr and N atoms corresponding to the C_1 configuration are given in Figs. 3 and 4, respectively. The total DOS for spin up and spin down is no longer identical around the Fermi level. The majority spin states (spin up) across the Fermi level show a metallic character, whereas the minority spin states (spin down) have a nearly vanishing band gap at the Fermi level and therefore exhibit a semimetallic character. The calculated local moments of Cr and N are $2.28\mu_B$ and $-0.07\mu_B$. In order to estimate the degree of polarization, we calculate the spin polarization P at the Fermi level given by $P=[n_\uparrow(E_F)-n_\downarrow(E_F)]/[n_\uparrow(E_F)+n_\downarrow(E_F)]$, where $n\uparrow(E_f)$ and $n\downarrow(E_f)$ are the majority and the minority DOSs at E_F, respectively. We found a polarization of 96%; thus, InCrN material would be useful for spin electronics since its spin polarization at the Fermi level is strong.

Figure 4 shows that there is a visible overlap between Cr $3d$ and N $2p$ states near the Fermi level, suggesting a strong interaction between them. Additionally, Fig. 5 shows the spin density distribution of the FM-C_1 configuration where the isosurface of the spin up region is mainly filled with Cr $3d$ and N p electrons, in which the polarized components are mainly concentrated around the Cr–N–Cr complex. Therefore, the hybridization between Cr $3d$ and N p electrons mediates the stable FM ordering.

[1]T. Dietl, H. Ohno, F. Matsukura, J. Cibert, and D. Ferrand, Science **287**, 1019 (2000).
[2]H. Munekata, H. Ohno, S. von Molnar, A. Segmüller, L. L. Chang, and L. Saki, Phys. Rev. Lett. **63**, 1849 (1989).
[3]H. Ohno, A. Shen, F. Matsukara, A. Oiwa, A. Endo, S. Katsumoto, and Y. Iye, Appl. Phys. Lett. **69**, 363 (1996).
[4]S. Dhar, O. Brandt, A. Trampert, L. Däweritz, K. J. Friedland, K. H. Ploog, J. Keller, B. Beschoten, and G. Güntherodt, Appl. Phys. Lett. **82**, 2077 (2003).
[5]S. E. Park, H.-J. Lee, Y. C. Cho, S.-Y. Jeong, C. R. Cho, and S. Cho, Appl. Phys. Lett. **80**, 4187 (2002).
[6]S. Y. Wu, H. X. Liu, L. Gu, R. K. Singh, L. Budd, M. van Schilfgaarde, M. R. McCartney, J. D. Smith, and N. Newman, Appl. Phys. Lett. **82**, 3047 (2003).
[7]S. Dhar, O. Brandt, M. Ramsteiner, V. F. Sapege, and K. H. Ploog, Phys. Rev. Lett. **94**, 037205 (2005).
[8]X. H. Ji, S. P. Lau, S. F. Yu, H. Y. Yang, T. S. Herng, A. Sedhain, J. Y. Lin, H. X. Jiang, K. S. Teng, and J. S. Chen, Appl. Phys. Lett. **90**, 193118 (2007).
[9]P. P. Chen, H. Makinoa, and T. Yao, J. Cryst. Growth **269**, 66 (2004).
[10]R. Rajaram, A. Ney, G. Solomon, J. S. Harris, Jr., R. F. C. Farrow, and S. S. P. Parkin, Appl. Phys. Lett. **87**, 172511 (2005).
[11]P. A. Anderson, R. J. Kinsey, S. M. Durbin, A. Markwitz, V. J. Kennedy, A. Asadov, W. Gao, and R. J. Reeves, J. Appl. Phys. **98**, 043903 (2005).
[12]A. Ney, R. Rajaram, E. Arenholz, J. S. Harris, Jr., M. Samant, R. F. C. Farrow, and S. S. P. Parkin, J. Magn. Magn. Mater. **300**, 7 (2006).
[13]R. Rajaram, A. Ney, R. F. C. Farrow, S. S. P. Parkin, G. S. Solomon, and J. S. Harris, Jr., J. Vac. Sci. Technol. B **24**, 1644 (2006).
[14]A. Ney, R. Rajaram, S. S. P. Parkin, T. Kammermeier, and S. Dhar, Phys. Rev. B **76**, 035205 (2007).
[15]B. S. Kang, H. Ki Lee, K. S. Kim, and H. J. Kang, Phys. Scr. **79**, 025701 (2009).
[16]J. P. Perdew, K. Burke, and M. Ernzerhof, Phys. Rev. Lett. **77**, 3865 (1996).
[17]S. Baroni, A. Dal Corso, A. S. de Gironcoli, and S. P. Giannozzi, http://www.pwscf.org.
[18]J. D. Pack and H. J. Monkhorst, Phys. Rev. B **16**, 1748 (1977).
[19]N. Marzari, D. Vanderbilt, A. De Vita, and M. C. Payne, Phys. Rev. Lett. **82**, 3296 (1999).
[20]H. Hellmann, *Einfuhrung in die Quantumchemie* (Franz Deutsche, Leipzig, 1937).
[21]R. P. Feynman, Phys. Rev. **56**, 340 (1939).
[22]M. Briki, A. Zaoui, F. Boutaiba, and M. Ferhat, Appl. Phys. Lett. **91**, 182105 (2007).
[23]L. G. Ferreira, M. Marques, and L. K. Teles, Phys. Rev. B **78**, 125116 (2008).
[24]G. Kresse and J. Furthmüller, Phys. Rev. B **54**, 11169 (1996).
[25]M. S. Hybertsen and S. G. Louie, Phys. Rev. Lett. **55**, 1418 (1985).
[26]J. Schörmann, D. J. As, K. Lischka, P. Schley, R. Goldhahn, S. F. Li, W. Löffler, M. Hetterich, and H. Kalt, Appl. Phys. Lett. **89**, 261903 (2006).